Geochemical Perspectives Letters

The vanadium isotope composition of Mars: implications for planetary differentiation in the early solar system

S.G. Nielsen[1,2*], D.V. Bekaert[1], T. Magna[3], K. Mezger[4], M. Auro[1]

doi: 10.7185/geochemlet.2032

Abstract

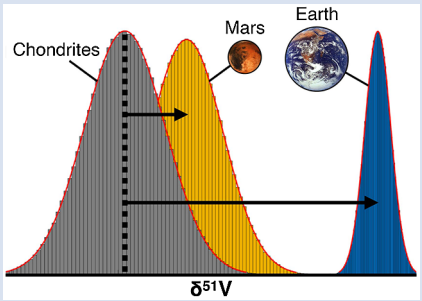

The V isotope composition of martian meteorites reveals that Bulk Silicate Mars (BSM) is characterised by $\delta^{51}V = -1.026 \pm 0.029$ ‰ (2 s.e.) and is thus ~0.06 ‰ heavier than chondrites and ~0.17 ‰ lighter than Bulk Silicate Earth (BSE). Based on the invariant V isotope compositions of all chondrite groups, the heavier V isotope compositions of BSE and BSM relative to chondrites are unlikely to originate from mass independent isotope effects or evaporation/condensation processes in the early Solar System. These differences are best accounted for by mass dependent fractionation during core formation. Assuming that bulk Earth and Mars both have a chondritic V isotopic compostion, mass balance considerations reveal V isotope fractionation factors $\Delta^{51}V_{core\text{-}mantle}$ as substantial as −0.6 ‰ for both planets. This suggests that V isotope systematics in terrestrial and extraterrestrial rocks potentially constitutes a powerful new tracer of planetary differentiation processes accross the Solar System.

Received 29 April 2020 | Accepted 29 June 2020 | Published 30 September 2020

Introduction

Vanadium is a refractory and moderately siderophile element with the two naturally occurring isotopes ^{51}V and ^{50}V. Variations of $^{51}V/^{50}V$ reported for terrestrial and extraterrestrial samples have been attributed to various processes, such as heterogeneous distribution of nucleosynthetically produced V (Nielsen *et al.*, 2019), kinetic and equilibrium mass dependent isotope fractionation during condensation from the protosolar nebula (Wu *et al.*, 2015; Nielsen *et al.*, 2019), early irradiation by solar irradiation (Lee *et al.*, 1998; Gounelle *et al.*, 2006; Sossi *et al.*, 2017), exposure of meteoroids to galactic cosmic rays (GCR) during their transition to Earth (Hopkins *et al.*, 2019), and/or magmatic differentiation (Prytulak *et al.*, 2017). Since V has only two isotopes, it is difficult to discriminate among the different processes that can lead to V isotope variations in geological material. Therefore, additional constraints are needed to interpret V isotope signatures in cosmochemical and geochemical contexts. To further explore the origin of $\delta^{51}V$ variations (where $\delta^{51}V_{sample} = (((^{51}V/^{50}V)_{sample}/(^{51}V/^{50}V)_{AA} - 1) \times 1000$, with AA being the Alfa Aesar reference solution) among terrestrial planets, a comprehensive set of V isotope data for martian meteorites was obtained. These data are compared with the value for chondrites of $\delta^{51}V = -1.089 \pm 0.029$ ‰ (2 s.e.) (see Supplementary Information) to provide additional constraints on potential accretionary sources for Mars, and to investigate the possible mechanisms of V isotope fractionation during planetary differentiation and igneous processes.

Results and Discussion

The 24 martian meteorites investigated here represent a petrologic range of shergottites (basaltic, olivine-phyric, lherzolitic), clinopyroxene-rich cumulates (nakhlites) and orthopyroxenite (Table 1). The measured $\delta^{51}V$ for martian meteorites display a rather restricted range of values from −1.25 to −0.89 ‰ (Table 1) with a mean of $\delta^{51}V = -1.043 \pm 0.034$ ‰ (2 s.e.). Due to their young exposure ages and relatively low Fe/V ratios most samples require very minor, if any, correction for spallation by GCR (see Supplementary Information). Corrected $\delta^{51}V$ values are all within error of each other and show no correlation with petrologic type or indicators of melting or fractional crystallisation (Fig. 1). Pooled data for the different martian meteorite groups yield indistinguishable mean $\delta^{51}V$ (Table 1; Supplementary Information), further supporting a limited effect of magmatic processes, such as partial melting and fractional crystallisation, on V isotopes. This inference is consistent with the absence of discernible, systematic $\delta^{51}V$ variations among terrestrial peridotites and basalts (see Supplementary Information), as well as lunar rock data corrected for GCR effects (Hopkins *et al.*, 2019).

Invariant V isotope compositions recorded in martian meteorites collectively indicate that BSM (and by analogy BSE) inherited its $\delta^{51}V$ signature during its accretion and/or differentiation history. Here, the GCR corrected and error weighted average V isotope composition of martian meteorites (Table 1) is used to derive the best estimate for the V isotope source signature of BSM, which yields $\delta^{51}V = -1.026 \pm 0.027$ ‰

1. NIRVANA Laboratories, Woods Hole Oceanographic Institution, Woods Hole, MA 02543, USA
2. Department of Geology and Geophysics, Woods Hole Oceanographic Institution, Woods Hole, MA 02543, USA
3. Czech Geological Survey, Klarov 3, CZ-11821 Prague, Czech Republic
4. Institut für Geologie and Center for Space and Habitability, Universität Bern, Baltzerstrasse 1+3, CH-3012 Bern, Switzerland
* Corresponding author (email: snielsen@whoi.edu)

Table 1 Vanadium isotope data for martian meteorites.

Sample	Fe[$] (mg/g)	V[$] (µg/g)	CRE age[¶] (Ma)	$\delta^{51}V_{meas}$	2 s.d.	splits	n	$\delta^{51}V_{corr}$[§]
Basaltic shergottites								
Los Angeles 001	**224**	**258**	3.0	−0.95	0.12	3	8	−0.94
NWA 856	**132**	**273**	2.6	−0.94	0.13	1	10	−0.94
NWA 4864	**153**	**325**	3.0	−1.11	0.23	3	8	−1.10
Shergotty	**173**	**310**	3.0	−0.89	0.19	2	8	−0.89
Zagami	*141*	*312*	3.0	−1.15	0.23	2	14	−1.14
				Error weighted group average				**−0.97**
Olivine-phyric shergottites								
EETA 79001 A	*143*	*210*	0.7	−1.02	0.19	2	6	−1.02
SaU 005	*143*	196	1.2	−1.12	0.24	2	14	−1.12
SaU 051	**150**	204	1.2	−1.03	0.21	2	11	−1.03
SaU 094	**149**	**212**	1.2	−1.11	0.20	2	4	−1.11
NWA 1068	**155**	**207**	2.8	−1.11	0.16	6	22	−1.10
LAR 06319	*159*	*202*	3.3	−1.04	0.16	2	5	−1.03
Y-980459	**144**	**213**	1.1	−1.00	0.09	1	4	−1.00
NWA 4925	**149**	**181**	0.6	−0.98	0.19	3	9	−0.98
NWA 6162	*142*	*112*	1.0	−0.90	0.15	1	4	−0.89
DaG476	**122**	**167**	1.0	−1.09	0.13	3	11	−1.09
RBT 04262	**201**	**212**	2.1	−1.04	0.06	1	3	−1.04
				Error weighted group average				**−1.03**
Lherzolitic shergottites								
ALH 77005	*156*	*162*	4.3	−1.11	0.12	3	11	−1.10
NWA 1950	*168*	140	4.1	−1.00	0.10	2	9	−0.99
Y-000097	*155*	*180*	4.6	−1.01	0.14	1	4	−1.00
				Error weighted group average				**−1.03**
Nakhlites								
Nakhla	*160*	*192*	11.6	−1.25	0.19	1	5	−1.23
MIL 03346	**137**	**195**	9.5	−1.08	0.14	2	6	−1.07
NWA 817	*154*	*181*	10.0	−0.98	0.15	1	2	−0.96
Y-000593	**117**	**125**	11.8	−1.03	0.22	1	7	−1.01
				Error weighted group average				**−1.06**
Orthopyroxenite								
ALH 84001	*136*	*201*	14.7	−1.09	0.15	1	4	−1.07
					Error weighted average Mars			**−1.026**
					2 s.e.			**0.027**
					MSWD			**0.991**

[$] Iron and V concentrations are either from the literature (in italics; Lodders, 1998; Dreibus *et al.*, 2000; Sautter *et al.*, 2002; Gillet *et al.*, 2005; Basu Sarbadhikari *et al.*, 2009; Shirai and Ebihara, 2009; Kuehner *et al.*, 2011), measured by ICPMS at WHOI (bold), or estimated based on yield during column chemistry.
[¶] CRE ages from Eugster *et al.* (2002), Mathew *et al.* (2003), Christen *et al.* (2005), Nagao and Park (2008), Nagao *et al.* (2008), Nishiizumi *et al.* (2011) and Wieler *et al.* (2016) except for NWA4864, which is assumed similar to the other basaltic shergottites.
[§] Vanadium isotope compositions corrected for spallogenic production of ^{50}V using the equation: $\delta^{51}V_{corr} = \delta^{51}V_{meas} + [Fe] \times CRE \times 2.1 \times 10^{-6}/[V]$ (Hopkins *et al.*, 2019).

(2 s.e., MSWD = 0.99). This value is markedly different from the mean $\delta^{51}V$ of BSE (−0.856 ± 0.020 ‰, 2 s.e.). Understanding the cause(s) of V isotope variations among terrestrial planets could potentially provide constraints on the accretion history and building blocks of Earth and Mars, as well as isotopic effects during planetary differentiation. In the following, we explore possible explanations for the V isotope difference between Mars and chondrites, and discuss the implications for how BSM and BSE could have acquired their V isotope compositions.

Whereas stable isotope systems such as Mg, Si, Ca, and Fe in martian samples (Armytage *et al.*, 2011; Magna *et al.*, 2015; Sossi *et al.*, 2016; Hin *et al.*, 2017; Magna *et al.*, 2017) show only limited, if any, deviations from chondritic values, large nucleosynthetic isotope anomalies have been observed for many other elements in chondrites and planetary materials including Mars (*e.g.*, ^{54}Cr, ^{50}Ti, ^{17}O, ^{62}Ni; Warren, 2011). Given that Mars likely accreted very rapidly and early relative to Earth (Dauphas and Pourmand, 2011), the V isotope difference between Mars and Earth could denote primary spatial variability and/or temporal evolution of the nucleosynthetic V isotope composition of planetary accretion source material in the inner Solar System (*e.g.*, Warren, 2011). However, although V isotope compositions of bulk carbonaceous chondrites have been proposed to correlate broadly with nucleosynthetic anomalies of ^{54}Cr (Nielsen *et al.*, 2019), subsequent studies have found that the V isotope

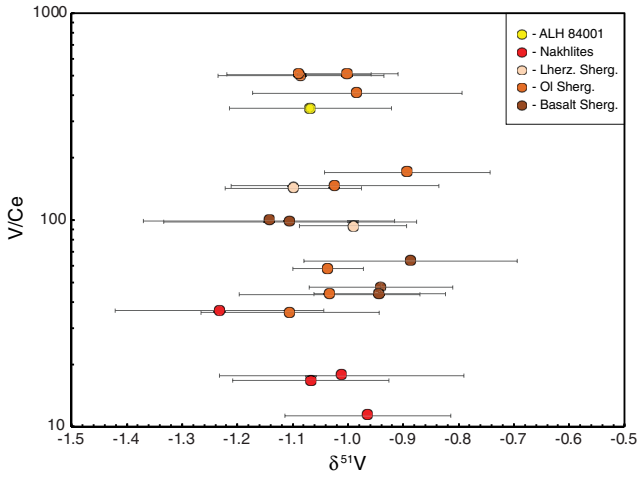

Figure 1 Martian meteorite vanadium isotopic data corrected for GCR effects plotted against V/Ce ratios. Error bars are 2 s.d. as listed in Table 1. Given that V and Ce have different partition coefficients during fractional crystallisation and melting, variations in V/Ce likely reflect a combination of these processes. The lack of systematic V isotope variation over the entire range of V/Ce implies that magmatic processes did not induce detectable V isotope variation on Mars. Ce concentrations from Yoshizaki and McDonough (2020); V concentrations from Table 1. Note log scale on y axis.

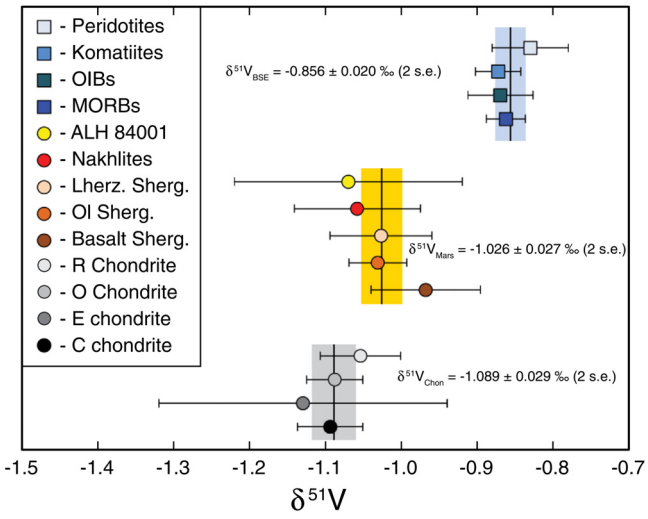

Figure 2 Vanadium isotope data for different sample types from the Solar System. Data for terrestrial samples are from Prytulak *et al.* (2013), Wu *et al.* (2018) and Qi *et al.* (2019); chondrite data are from Nielsen *et al.*, (2019) and this study (Table S-2). All data have been corrected for spallation-produced ^{50}V. Error bars for each sample group are 2 s.e. weighted by the individual sample error bars shown in Table 1. Shaded areas denote the average for those objects and error weighted 2 s.e. of the entire data population. Chondrite averages have been weighted by individual measurement errors.

variation in bulk chondrites can be ascribed to recent production of ^{50}V from GCR spallation processes (Hopkins *et al.*, 2019). Carbonaceous, ordinary, enstatite and Rumuruti chondrite data corrected for this effect all display uniform $\delta^{51}V = -1.089 \pm 0.029$ ‰ (n = 14, 2 s.e.; see Supplementary Information). The lack of V isotope variation in chondrites compared with the large variations in *e.g.*, ^{54}Cr and ^{50}Ti implies that nucleosynthetic V isotope anomalies, if they exist, are unlikely to induce planetary scale V isotope heterogeneity. Similarly, irradiation processes are unlikely to account for planetary V isotope variations given the large abundance variations of CAIs, the most likely carriers of irradiation-induced V isotope anomalies (Sossi *et al.*, 2017), in chondrites that display uniform bulk V isotope compositions. For these reasons, V isotope variations among terrestrial planets most likely do not reflect disparities in the signatures of their accretionary materials, but are the result of planetary processes.

Although BSE has a markedly heavier composition than other solar system bodies, there are still analytically significant differences between BSM and chondrites (Fig. 2). Two sample *t* tests demonstrate that the datasets of the BSM and chondrites are characterised by statistically distinct means (see Supplementary Information). Monte Carlo simulations using the raw datasets of the BSM and chondrites that include the individual sample errors show that there exists a difference of 0.058 ± 0.051 ‰ (1 s.d.) between these two populations, with a probability of ~87 % that the V isotope composition of the BSM is heavier than that of chondrites. Using the mean $\delta^{51}V$ compositions of the BSM and chondrites, instead of the raw data, to compute these Monte Carlo simulations yields a systematic difference of 0.067 ± 0.042 ‰ (1 s.d.) between BSM and chondrites. In the likely absence of mass independent V isotope effects (nucleosynthetic or irradiation-related) on the planetary scale, we propose that the most straightforward explanation for the V isotope disparity between differentiated (Earth, Mars) and non-differentiated (chondrites) bodies corresponds to small but non-negligible isotopic fractionation during core formation.

Considering that (i) the martian core comprises ~18 % by mass of the planet (Yoshizaki and McDonough, 2020), (ii) ~27–60 % of martian V resides in the core (see Supplementary Information), and (iii) $\Delta^{51}V_{BSM\text{-}chondrites} = 0.067 \pm 0.042$ ‰, the martian core should be characterised by $\delta^{51}V \sim -1.11$ to −1.38 ‰. This requires a metal-silicate isotope fractionation factor of $\Delta^{51}V_{core\text{-}mantle} = -0.04$ to −0.40 ‰ (Fig. 3). Regarding BSE, it is generally assumed that the main phase of metal segregation during terrestrial core formation readily accounts for the depletion of V in the silicate Earth (O'Neill, 1991; Chabot and Agee, 2003; Wade and Wood, 2005), with 40–50 % of terrestrial V now residing in the core (*e.g.*, Wade and Wood, 2005). If bulk Earth is taken to be chondritic for V isotopes, then mass balance dictates that the core is characterised by $\delta^{51}V = -1.39 \pm 0.10$ ‰,

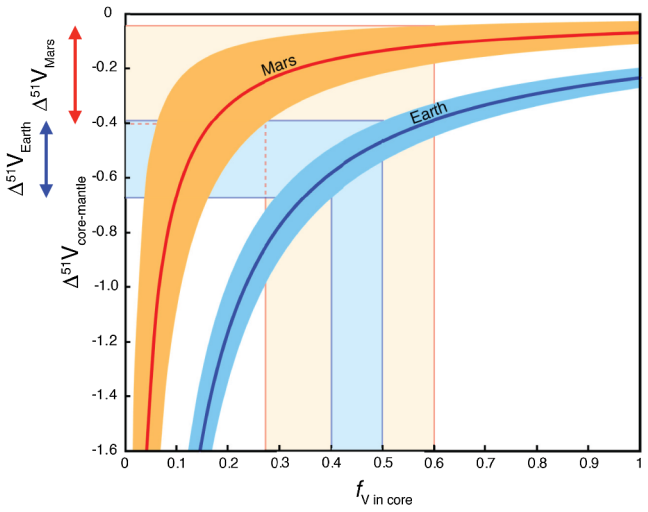

Figure 3 Modelled V isotope fractionation factors between the core and mantle of Earth (blue) and Mars (red) as a function of the fraction of total V that entered the core.

which corresponds to a metal-silicate isotope fractionation factor of $\Delta^{51}V_{core\text{-}mantle} = -0.53 \pm 0.14$ ‰ (using $\Delta^{51}V_{BSE\text{-}chondrites} = 0.233 \pm 0.037$ ‰, 2 s.e.). This value is somewhat larger than that required to explain the BSM–chondrite V isotope offset (Fig. 3), which could imply variations in V isotope fractionation during planetary differentiation.

The metal-silicate isotope fractionation factor required to satisfy V geochemical constraints ($\Delta^{51}V_{metal\text{-}silicate}$ up to −0.6 ‰) is substantially larger than values found for other redox sensitive stable isotope systems like Mo, Fe and Cr (all <0.1 ‰; Hin *et al.* (2013), Bonnand *et al.* (2016), and Elardo *et al.*, (2019)). A small core–mantle isotope fractionation factor for V is also suggested by the only available investigation of V isotope fractionation during metal–silicate partitioning, where experiments at 1.5 GPa and ~1900 K revealed no detectable V isotope fractionation outside the analytical uncertainty (~±0.2 ‰; Nielsen *et al.*, 2014). However, Earth's core likely formed through a complex, multi-stage process, starting as a reduced body that gradually evolved to more oxidised as Earth grew (*e.g.*, Wade and Wood, 2005), with a final stage of core segregation in the form of immiscible metal and sulfide melts after the Moon-forming giant impact (*e.g.*, O'Neill, 1991). Additional experiments of V isotopic partitioning at higher pressure-temperature conditions, for variable oxygen fugacities and/or chemical compositions (*e.g.*, presence or not of light elements and other metal alloys) are needed to test the hypothesis of V isotope fractionation during core formation. Such effects have, for example, been observed for Fe isotopes (Elardo *et al.*, 2019). Notably, the sensitivity of V valence state to the oxygen fugacity during core formation offers a promising alternative for potentially inducing significant V isotope fractionation during metal-silicate partitioning. For example, the oxygen fugacity during core formation on Mars and Earth were likely different (Wood *et al.*, 2006) and may have been a contributing factor in the apparent V isotope fractionation difference between these two planets.

One outstanding challenge is to explain the strikingly heavy V isotope composition of BSE compared to BSM. Future experimental investigations may shed light on the possibility for higher temperatures and pressures during terrestrial core formation, and/or late segregation of the Hadean matte (which seemingly did not happen on Mars) to account for this difference. Based on current constraints, it appears that the late stage sulfide segregation on Earth is unlikely to have removed substantial amounts of V to the core (*e.g.*, Wade and Wood, 2005). We, therefore, consider that the heavy V isotope composition of BSE was most likely established during the main phase of core segregation, before Moon formation. Alternative avenues of investigation to explain the heavy V isotope composition of BSE and BSM may require unusual isotope fractionation processes to operate at the core–mantle boundary, as recently proposed for Fe in the case of thermodiffusion (Lesher *et al.*, 2020). Nonetheless, we speculate that identifying the process(es) responsible for V isotope variations in terrestrial planets will ultimately allow better understanding the conditions of planetary differentiation in the Solar System.

Acknowledgements

This work was funded by NASA Emerging Worlds grant NNX16AD36G to SGN. Samples were acquired with funds from the Helmholtz Association through the research alliance HA 203 "Planetary Evolution and Life" to KM. TM contributed through the Strategic Research Plan of the Czech Geological Survey (DKRVO/ČGS 2018-2022). KM acknowledges support through NCCR PlanetS supported by the Swiss National Science Foundation. We thank Jurek Blusztajn for support in the WHOI Plasma Facility.

Editor: Anat Shahar

Additional Information

Supplementary Information accompanies this letter at http://www.geochemicalperspectivesletters.org/article2032.

Cite this letter as: Nielsen, S.G., Bekaert, D.V., Magna, T., Mezger, K., Auro, M. (2020) The vanadium isotope composition of Mars: implications for planetary differentiation in the early solar system. *Geochem. Persp. Let.* 15, 35–39.

References

Armytage, R.M.G., Georg, R.B., Savage, P.S., Williams, H.M., Halliday, A.N. (2011) Silicon isotopes in meteorites and planetary core formation. *Geochimica et Cosmochimica Acta* 75, 3662–3676.

Basu Sarbadhikari, A., Day, J.M.D., Liu, Y., Rumble, D., Taylor, L.A. (2009) Petrogenesis of olivine-phyric shergottite Larkman Nunatak 06319: implications for enriched components in martian basalts. *Geochimica et Cosmochimica Acta* 73, 2190–2214.

Bonnand, P., Williams, H.M., Parkinson, I.J., Wood, B.J., Halliday, A.N. (2016) Stable chromium isotopic composition of meteorites and metal-silicate experiments: Implications for fractionation during core formation. *Earth and Planetary Science Letters* 435, 14–21.

Chabot, N.L., Agee, C.B. (2003) Core formation in the Earth and Moon: New experimental constraints from V, Cr, and Mn. *Geochimica et Cosmochimica Acta* 67, 2077–2091.

Christen, F., Eugster, O., Busemann, H. (2005) Mars ejection times and neutron capture effects of the nakhlites Y000593 and Y000749, the olivine-phyric shergottite Y980459, and the lherzolite NWA1950. *Antarctic Meteorite Research* 18, 117–132.

Dauphas, N., Pourmand, A. (2011) Hf-W-Th evidence for rapid growth of Mars and its status as a planetary embryo. *Nature* 473, 489–U227.

Dreibus, G., Spettel, B., Haubold, R., Jochum, K.P., Palme, H., Wolf, D., Zipfel, J. (2000) Chemistry of a new shergottite: Sayh al Uhaymir 005. *Meteoritics and Planetary Science* 35, A49.

Elardo, S.M., Shahar, A., Mock, T.D., Sio, C.K. (2019) The effect of core composition on iron isotope fractionation between planetary cores and mantles. *Earth and Planetary Science Letters* 513, 124–134.

Eugster, O., Busemann, H., Lorenzetti, S., Terribilini, D. (2002) Ejection ages from krypton-81-krypton-83 dating and pre-atmospheric sizes of martian meteorites. *Meteoritics & Planetary Science* 37, 1345–1360.

Gillet, P., Barrat, J.A., Beck, P., Marty, B., Greenwood, R.C., Franchi, I.A., Bohn, M., Cotten, J. (2005) Petrology, geochemistry, and cosmic-ray exposure age of lherzolitic shergottite Northwest Africa 1950. *Meteoritics & Planetary Science* 40, 1175–1184.

Gounelle, M., Shu, F.H., Shang, H., Glassgold, A.E., Rehm, K.E., Lee, T. (2006) The irradiation origin of beryllium radioisotopes and other short-lived radionuclides. *Astrophysical Journal* 640, 1163–1170.

Hin, R.C., Burkhardt, C., Schmidt, M.W., Bourdon, B., Kleine, T. (2013) Experimental evidence for Mo isotope fractionation between metal and silicate liquids. *Earth and Planetary Science Letters* 379, 38–48.

Hin, R.C., Coath, C.D., Carter, P.J., Nimmo, F., Lai, Y.-J., Pogge von Strandmann, P.A.E., Willbold, M., Leinhardt, Z.M., Walter, M.J., Elliott, T. (2017) Magnesium isotope evidence that accretional vapour loss shapes planetary compositions. *Nature* 549, 511.

Hopkins, S.S., Prytulak, J., Barling, J., Russell, S.S., Coles, B.J., Halliday, A.N. (2019) The vanadium isotopic composition of lunar basalts. *Earth and Planetary Science Letters* 511, 12–24.

Kuehner, S.M., Irving, A.J., Herd, C.D.K., Gellissen, M., Lapen, T.J., Rumble, D. (2011) Pristine olivine-phyric shergottite Northwest Africa 6162: a primitive magma with accumulated crystals derived from depleted martian mantle. *42nd Lunar and Planetary Science Conference*, The Woodlands, Texas. 1610.

Lee, T., Shu, F.H., Shang, H., Glassgold, A.E., Rehm, K.E. (1998) Protostellar cosmic rays and extinct radioactivities in meteorites. *Astrophysical Journal* 506, 898–912.

Lesher, C.E., Dannberg, J., Barfod, G.H., Bennett, N.R., Glessner, J.J.G., Lacks, D.J., Brenan, J.M. (2020) Iron isotope fractionation at the core–mantle boundary by thermodiffusion. *Nature Geoscience* 13, 382–386.

Lodders, K. (1998) A survey of shergottite, nakhlite and chassigny meteorites whole-rock compositions. *Meteoritics & Planetary Science* 33, A183–A190.

Magna, T., Gussone, N., Mezger, K. (2015) The calcium isotope systematics of Mars. *Earth and Planetary Science Letters* 430, 86–94.

Magna, T., Hu, Y., Teng, F.-Z., Mezger, K. (2017) Magnesium isotope systematics in Martian meteorites. *Earth and Planetary Science Letters* 474, 419–426.

Mathew, K.J., Marty, B., Marti, K., Zimmermann, L. (2003) Volatiles (nitrogen, noble gases) in recently discovered SNC meteorites, extinct radioactivities and evolution. *Earth and Planetary Science Letters* 214, 27–42.

Nagao, K., Park, J. (2008) Noble gases and cosmic-ray exposure ages of two Martian shergottites, RBT 04262 and LAR 06319, recovered in Antarctica. *71st Annual Meteoritical Society Meeting*, Matsue, Japan. 5200.

Nagao, K., Park, J., Choi, H.G. (2008) Noble gases of the Yamato 000027 and Yamato 000097 lherzolitic shergottites from Mars. *Polar Science* 2, 195–214.

Nielsen, S.G., Prytulak, J., Wood, B.J., Halliday, A.N. (2014) Vanadium isotopic difference between the silicate Earth and meteorites. *Earth and Planetary Science Letters* 389, 167–175.

Nielsen, S.G., Auro, M., Righter, K., Davis, D., Prytulak, J., Wu, F., Owens, J.D. (2019) Nucleosynthetic vanadium isotope heterogeneity of the early solar system recorded in chondritic meteorites. *Earth and Planetary Science Letters* 505, 131–140.

Nishiizumi, K., Nagao, K., Caffee, M.W., Jull, A.J.T., Irving, A.J. (2011) Cosmic-ray exposure chronologies of depleted olivine-phyric shergottites. *42nd Lunar and Planetary Science Conference*, The Woodlands, Texas. 2371.

O'Neill, H.S.C. (1991) The origin of the moon and the early history of the earth – A chemical model. Part 2: The earth. *Geochimica et Cosmochimica Acta* 55, 1159–1172.

Prytulak, J., Nielsen, S.G., Ionov, D.A., Halliday, A.N., Harvey, J., Kelley, K.A., Niu, Y., Peate, D.W., Shimizu, K., Sims, K.W.W. (2013) The Stable Vanadium Isotope Composition of the Mantle and Mafic Lavas. *Earth and Planetary Science Letters* 365, 177–189.

Prytulak, J., Sossi, P.A., Halliday, A.N., Plank, T., Savage, P.S., Woodhead, J.D. (2017) Stable vanadium isotopes as a redox proxy in magmatic systems? *Geochemical Perspectives Letters* 3, 75–84.

Qi, Y.H., Wu, F., Ionov, D.A., Puchtel, I.S., Carlson, R.W., Nicklas, R.W., Yu, H.M., Kang, J.T., Li, C.H., Huang, F. (2019) The vanadium isotopic composition of the BSE: constraints from peridotites and komatiites. *Geochimica et Cosmochimica Acta* 259, 288–301.

Sautter, V., Barrat, J.A., Jambon, A., Lorand, J.P., Gillet, P., Javoy, M., Loron, J.L., Lesourd, M. (2002) A new Martian meteorite from Morocco: the nakhlite North West Africa 817. *Earth and Planetary Science Letters* 195, 223–238.

Shirai, N., Ebihara, M. (2009) Chemical characteristics of the lherzolitic shergottite Yamato 000097: magmatism on Mars inferred from the chemical compositions of shergottites. *Polar Science* 3, 117–133.

Sossi, P.A., Nebel, O., Anand, M., Poitrasson, F. (2016) On the iron isotope composition of Mars and volatile depletion in the terrestrial planets. *Earth and Planetary Science Letters* 449, 360–371.

Sossi, P.A., Moynier, F., Chaussidon, M., Villeneuve, J., Kato, C., Gounelle, M. (2017) Early Solar System irradiation quantified by linked vanadium and beryllium isotope variations in meteorites. *Nature Astronomy* 1, 0055.

Wade, J., Wood, B.J. (2005) Core formation and the oxidation state of the Earth. *Earth and Planetary Science Letters* 236, 78–95.

Warren, P.H. (2011) Stable-isotopic anomalies and the accretionary assemblage of the Earth and Mars: A subordinate role for carbonaceous chondrites. *Earth and Planetary Science Letters* 311, 93–100.

Wieler, R., Huber, L., Busemann, H., Seiler, S., Leya, I., Maden, C., Masarik, J., Meier, M.M.M., Nagao, K., Trappitsch, R., Irving, A.J. (2016) Noble gases in 18 Martian meteorites and angrite Northwest Africa 7812—Exposure ages, trapped gases, and a re-evaluation of the evidence for solar cosmic ray produced neon in shergottites and other achondrites. *Meteoritics & Planetary Science* 51, 407–428.

Wood, B.J., Walter, M.J., Wade, J. (2006) Accretion of the Earth and segregation of its core. *Nature* 441, 825–833.

Wu, F., Qi, Y., Perfit, M.R., Gao, Y., Langmuir, C.H., Wanless, V.D., Yu, H., Huang, F. (2018) Vanadium isotope compositions of mid-ocean ridge lavas and altered oceanic crust. *Earth and Planetary Science Letters* 493, 128–139.

Wu, F., Qin, T., Li, X.F., Liu, Y., Huang, J.H., Wu, Z.Q., Huang, F. (2015) First-principles investigation of vanadium isotope fractionation in solution and during adsorption. *Earth and Planetary Science Letters* 426, 216–224.

Yoshizaki, T., McDonough, W.F. (2020) The composition of Mars. *Geochimica et Cosmochimica Acta* 273, 137–162.

Geochemical Perspectives Letters

The vanadium isotope composition of Mars: implications for planetary differentiation in the early solar system

S.G. Nielsen, D.V. Bekaert, T. Magna, K. Mezger, M. Auro

Supplementary Information

The Supplementary Information includes:

1. Methods

Powdered samples (30–90 mg) were dissolved using double-distilled concentrated HF, HNO_3, and HCl. Vanadium was separated from the sample matrix using a four-step cation/anion exchange chromatography procedure described in detail elsewhere (Nielsen *et al.*, 2011, 2019). Briefly, the method comprises one cation exchange resin column in 1M HNO_3, followed by three anion exchange resin columns where V is bound to the resin by complexation with H_2O_2 (Nielsen *et al.*, 2011). Throughout the study chemical yields were >80% and were monitored for by comparing the mass of V recovered from the ion exchange chemistry with the amount of V processed, which was based on either V concentrations measured in each sample or collected from literature data. Blanks were monitored with each batch of samples and were always <2 ng, which is insignificant compared with the >1000 ng V processed for each sample.

Vanadium isotope ratios were measured using a Neptune multiple-collector inductively-coupled-plasma mass spectrometer (MC-ICPMS), housed at the Plasma Mass Spectrometry Facility of the Woods Hole Oceanographic Institution (WHOI). Isotope compositions were determined using standard–sample bracketing with the Alfa Aesar reference solution that is defined as $\delta^{51}V = 0‰$ (Nielsen *et al.*, 2011). Each unknown sample was interspersed with a pure V reference solution from BDH Chemicals that has now been measured in eight separate studies with the identical

$\delta^{51}V = -1.18 \pm 0.02$‰ (2SE) (Nielsen *et al.*, 2011; Wu *et al.*, 2016; Prytulak *et al.*, 2017; Schuth *et al.*, 2017; Sossi *et al.*, 2017; Nielsen *et al.*, 2019; Wu *et al.*, 2019). The mass spectrometer was operated in medium resolution mode. To quantify and correct for isobaric interferences of ^{50}Ti and ^{50}Cr on ^{50}V the masses ^{48}Ti, ^{49}Ti, ^{52}Cr and ^{53}Cr were monitored and a mass bias correction routine using ^{49}Ti/^{50}Ti and ^{53}Cr/^{50}Cr ratios was applied (Nielsen *et al.*, 2016; Wu *et al.*, 2016). Mass ^{51}V was collected using a Faraday cup equipped with a 10^{10} Ω resistor, whereas Faraday cups with conventional 10^{11} Ω resistors were used to collect all other masses. Samples and standards were measured at a concentration of 800 ng/ml V, which produced an ion beam of ~2 nA on ^{51}V and ~0.005 nA on ^{50}V. Precision and accuracy of the V isotope measurements was assessed by measuring the BDH standard throughout the study (covering the period from February 2015 to September 2018) and by processing USGS reference materials AGV-2 and BCR-2 with every batch of unknown samples. These reference materials have previously been analyzed by different laboratories (Nielsen *et al.*, 2019). The resulting mean $\delta^{51}V$ values for AGV-2 and BCR-2 for the entire analytical period were -0.73 ± 0.15‰ (2SD; n = 47) and -0.83 ± 0.20‰ (2SD; n = 65), respectively, which is in excellent agreement with previous studies (Prytulak *et al.*, 2011, 2013; Wu *et al.*, 2016, 2018; Nielsen *et al.*, 2019). These external errors are similar to those obtained for the martian meteorites that exhibit 2SD from 0.06 to 0.24‰ (Table 1).

Elemental concentrations were determined for a subset of the samples using a ThermoFinnigan iCap quadrupole ICP-MS, housed at the WHOI Plasma Mass Spectrometry Facility. Concentrations were calculated via reference to ion beam intensities obtained from a five-point calibration curve constructed from serial dilutions of a gravimetrically-prepared multi-element standard; drift was monitored and corrected via normalization to indium intensities. Accuracy and precision were better than ± 7% (2SE) based on the correspondence of concentrations in USGS reference materials AGV-2, BCR-2, and BHVO-2 determined during the same analytical sessions as the martian meteorites.

2. Uniformity of the V isotope composition of martian rocks

Previous studies have demonstrated that GCR spallation produces ^{50}V, which in some cases can be critical to correct for (Hopkins *et al.*, 2019). All the martian meteorites investigated here have relatively young cosmic ray exposure ages (<15 Ma for nakhlites and ALH84001, <5 Ma for shergottites (e.g. Nyquist *et al.*, 2001)) and, compared with most other meteorites from different parent bodies, relatively high V contents, which results in corrections for GCR spallation of <0.03‰ (Table 1). These corrections are based on the correlations between cosmic ray exposure (CRE) ages and V isotope compositions of lunar rocks (Hopkins *et al.*, 2019). Application of the lunar rock calibration curve to other types of meteorites can be associated with significant systematic errors. However, given the very small total GCR corrections required for martian meteorites, it can be concluded that the corrections, as implemented here, are unlikely to induce any additional error on the V isotope compositions, because the average spallation correction for all martian meteorites is <0.01‰.

After correction for spallation effects, we investigated possible V isotope variations within the V isotope dataset for martian meteorites. These were performed by carrying out Monte Carlo simulations using the raw data and their associated uncertainties to artificially generate 1 million datasets for basaltic shergottites, olivine-phyric shergottites, lherzolitic shergottites, nakhlites and orthopyroxenite, and hence compute 1 million $\delta^{51}V$ mean values for each type of rocks. At each iteration step, the mean composition of olivine-phyric shergottites is compared to that of the other rocks ($\Delta^{51}V_{Ops\text{-}Smpl} = \delta^{51}V_{Ops} - \delta^{51}V_{Smpl}$, where "Ops" and "Smpl" correspond to olivine-phyric shergottites and other rock samples, respectively). Olivine-phyric shergottites were chosen here for reference, as they are the type of martian meteorites for which we have analyzed the most samples (and so for which we have the best statistics). Computed $\Delta^{51}V_{Ops\text{-}Smpl}$ are shown in Figure S-1, demonstrating that the V isotope composition of basaltic shergottites, lherzolitic shergottites, nakhlites and orthopyroxenite are statistically indistinguishable from that of olivine-phyric shergottites. The error-weighted average V isotope composition measured for the 24 martian meteorites is hence used to derive the best estimate for the V isotope composition of Bulk Silicate Mars (BSM), which yields $\delta^{51}V = -1.026 \pm 0.029$‰ (2SE, MSWD=0.99).

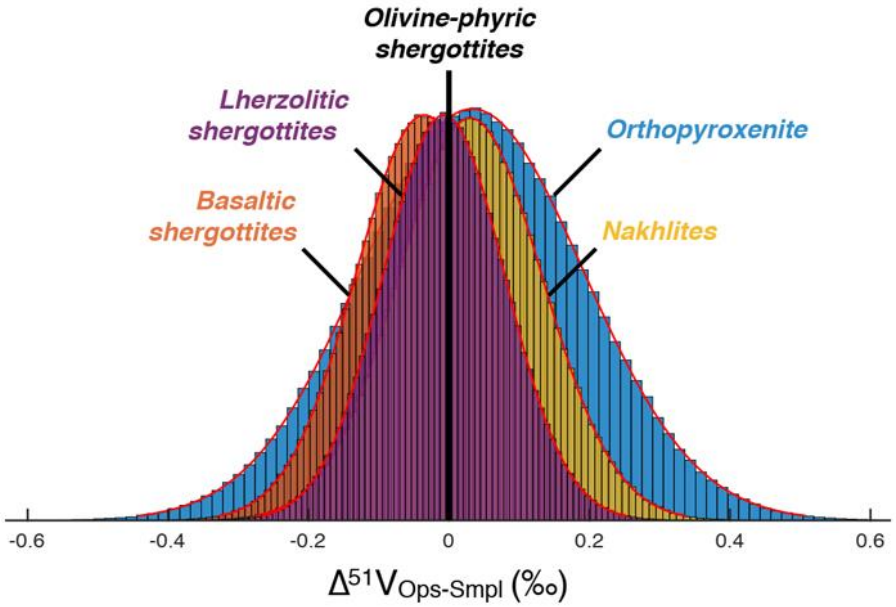

Figure S-1 Mean V isotope compositions of basaltic shergottites, lherzolitic shergottites, nakhlites and orthopyroxenite compared to that of olivine-phyric shergottites ($\Delta^{51}V_{Ops\text{-}Smpl}$) as generated by our Monte Carlo simulations (1 million runs).

Calculation of an average value for BSM and application of the 2SE uncertainty to this number requires that all individual data (i) originate from a unique population and (ii) are normally distributed around the mean (real) value of the population. To ascertain whether the martian data have come from a normally distributed population, we present a quantile-quantile (Q-Q) plot of the martian V isotope data (Fig. S-2). This plot corresponds to a graphical method for comparing two probability distributions - here the quantiles of the sample datasets versus theoretical quantile values generated from normal distributions - by plotting their quantiles against each other. The fact that the data broadly plot along a straight line in this Q-Q plot indicates that the martian V isotope dataset is consistent with a Gaussian distribution. However, these graphical considerations do not allow quantitatively validating/refuting the hypothesis of the dataset being normally distributed, and further statistical tests are required.

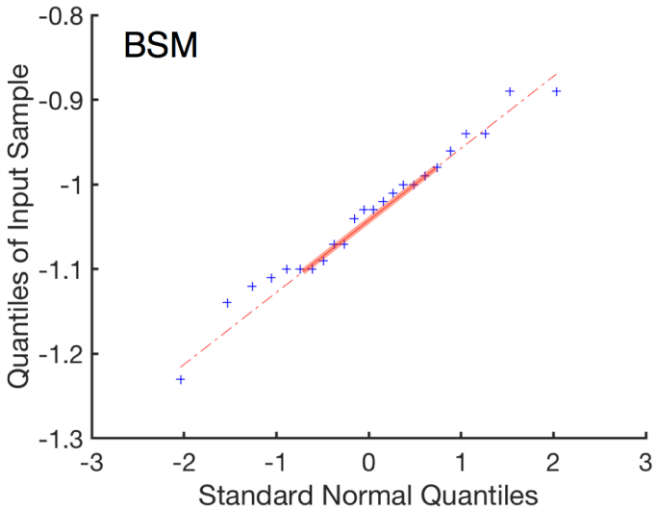

Figure S-2 Results of quantile-quantile calculations with the quantiles of the sample dataset plotted against theoretical quantile values generated from normal distributions. The linear relationship implies that the martian V isotope data are consistent with a normally distributed data population.

To further investigate whether the martian data have come from a normally distributed population, a series of Anderson-Darling normality tests was performed using the same Monte Carlo approach as for the Student's t-test. The Monte Carlo approach was chosen because Anderson-Darling and Student's t-tests are only based on the distribution of the data and do not take into account uncertainties associated with each individual datapoint. In order to overcome this caveat and compensate for the small size of the datasets, we used Monte Carlo simulations to artificially generate 1 million datasets for the BSM from the raw data and associated uncertainties. For each dataset, we postulate the null hypothesis that the generated dataset is from a population with a normal distribution. The Anderson-Darling test then returns a decision for the null hypothesis at the 5% significance level. After 1 million iterations, it is found that 90.5% of the tests did not reject the null hypothesis of normality, which further supports the conclusion that our data set is part of a normally distributed population.

3. V isotope composition of bulk silicate Earth

It has previously been argued that mantle melting on Earth might induce V isotope fractionation towards both lighter and heavier compositions (Prytulak *et al.*, 2013; Qi *et al.*, 2019). Therefore, it was suggested that fertile peridotites were the most appropriate samples to use for estimating the V isotope composition of the bulk silicate Earth (BSE) (Prytulak *et al.*, 2013; Qi *et al.*, 2019). However, this conclusion is at odds with the fact that both fertile and strongly melt depleted peridotites are indistinguishable in terms of V isotopes (Qi *et al.*, 2019), which would imply no detectable V isotope fractionation during melting. Likewise, extensive fractional crystallization does impart significant V isotope fractionation (Prytulak *et al.*, 2017), in particular if magnetite is removed from the melt during crystallization (Prytulak *et al.*, 2017; Sossi *et al.*, 2018). However, there is no evidence to suggest that V isotopes are fractionated during removal of early crystallizing phases such as olivine, orthopyroxene and clinopyroxene.

Figure S-3 shows the Probability Density Functions (PDF) of $\delta^{51}V$ for all available literature data on terrestrial rocks (Table S-1), which are then compared to each other in Figure S-4. When compiling all data from unaltered peridotites ($\delta^{51}V = -0.829 \pm 0.050$; n = 22, 2SE), unaltered mid ocean ridge basalts (MORBs) ($\delta^{51}V = -0.862 \pm 0.026$; n = 29, 2SE), komatiites ($\delta^{51}V = -0.872 \pm 0.030$; n = 14, 2SE), and ocean island basalts (OIBs) ($\delta^{51}V = -0.870 \pm 0.044$; n = 11; 2SE), it becomes clear that peridotites are indistinguishable from mantle melts and, therefore, all of these samples should be included in the best estimate for the BSE composition. This finding is notably underscored by Student's t-tests giving p-values of 0.25, 0.23, and 0.15 when peridotites are compared with MORBs, OIBs, and komatiites, respectively (Table S-1).

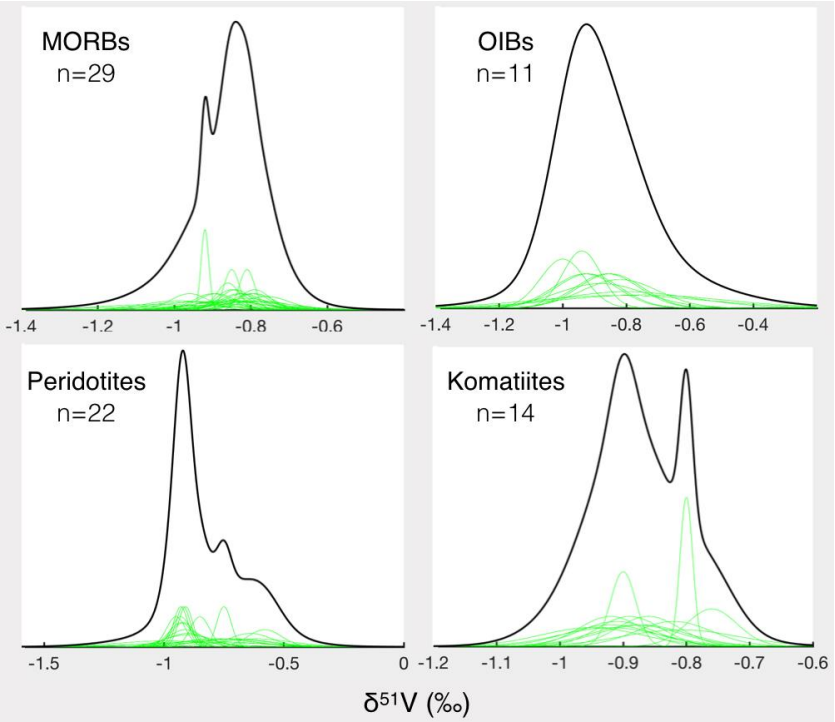

Figure S-3 PDF of $\delta^{51}V$ for all available literature data on terrestrial rocks (Table S-1). The numbers of samples (n) are reported for each type of terrestrial rock considered here.

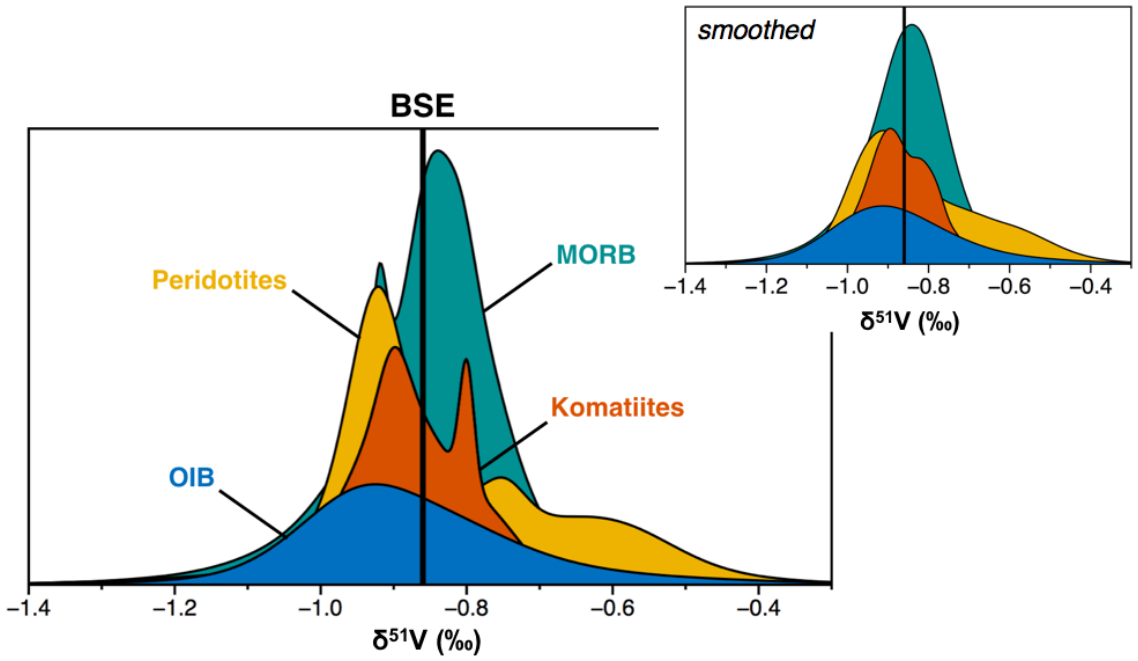

Figure S-4 Summary plot of the PDF of $\delta^{51}V$ for the four types of terrestrial rock considered here. Our computed mean composition of the BSE is reported as a vertical black line. The top right subpanel shows a smoothed version of these PDF.

In order to compensate for the limited size of our datasets and provide a meaningful statistical assessment of potential V isotope variations across terrestrial rocks, we carried out Monte Carlo simulations using the raw data and

their associated uncertainties to artificially generate 1 million datasets for peridotites, MORBs, komatiites and OIBs, and hence compute 1 million $\delta^{51}V$ mean values for each rock type. At each iteration step, the mean compositions of peridotites, komatiites and OIBs are compared to that of MORBs ($\Delta^{51}V_{MORB\text{-}Res.} = \delta^{51}V_{MORB} - \delta^{51}V_{Res.}$, where "Res." corresponds to peridotites, komatiites or OIBs). Computed $\Delta^{51}V_{MORB\text{-}res.}$ are shown in Figure S5, altogether with the 1SD envelope of the MORB mean value obtained for the 1 million runs. Here again, it appears that peridotites, komatiites and OIBs are statistically indistinguishable from MORBs (Figure S-5).

We therefore conclude that, even though it is possible that V isotopes are fractionated to some extent during mantle melting, current literature data as a whole do not demonstrate this process to operate. Therefore, it appears reasonable to compile all currently available V isotope data for relatively primitive mantle melts and peridotites that have not been significantly hydrothermally altered to obtain a more robust estimate for BSE, covering wide ranges of geographic dispersion, degrees of melting, as well as mantle source regions. All together we include 76 samples in our compilation (Prytulak *et al.*, 2011, 2013; Wu *et al.*, 2016, 2018; Qi *et al.*, 2019) (Table S1) and obtain an average value for BSE of $\delta^{51}V_{BSE} = -0.856 \pm 0.020$‰ (2SE). It is worth noting that this value is within error of previous estimates for BSE (Prytulak *et al.*, 2013; Qi *et al.*, 2019), but given the larger and more robust data set used here, it is much more precise.

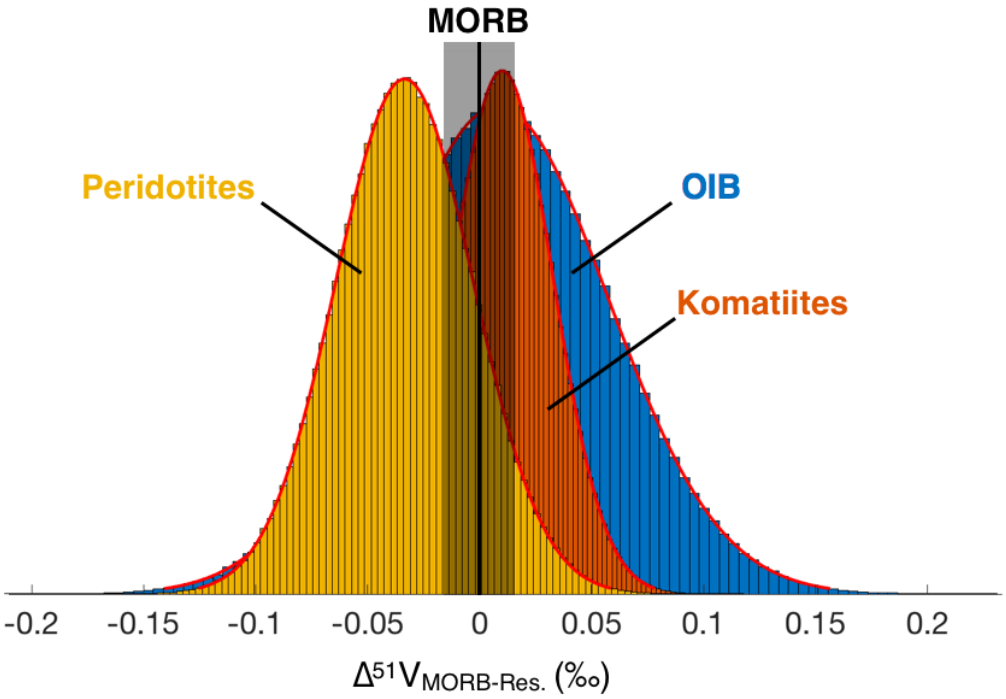

Figure S-5 Mean V isotope compositions of peridotites, komatiites and OIBs compared to that of MORBs ($\Delta^{51}V_{MORB\text{-}Res.}$) as generated by our Monte Carlo simulations (1 million runs). The mean and 1SD envelope of the MORB $\delta^{51}V_{MORB}$ as derived from these Monte Carlo simulations are reported as a vertical line and grey area, respectively.

Although the present estimate for BSE consists of a relatively large data set, it is still possible that some V isotopic heterogeneity exists in the Earth's mantle that has not yet been discovered. For example, early magma ocean crystallization on Earth could potentially have induced significant V isotope fractionation. Although mantle convection over Earth history is likely to have erased most of such potential variation, remnant isotopic heterogeneities inherited from early Earth processes clearly remain for some elements other than vanadium (Rizo *et al.*, 2016). Most likely, such variation would be found in the deep mantle that is much more sporadically sampled than the uppermost portion of the mantle, from which MORBs and most peridotites derive. However, the present estimate of the V isotope composition of BSE does include OIBs and komatiites that both sample deeper portions of the mantle. These data do not support the

existence of significant V isotopic heterogeneity in the deep mantle, therefore strengthening the case for our $\delta^{51}V_{BSE}$ estimate to be representative of the BSE composition.

4. V isotope composition of chondrites

Although chondrites on average exhibit relatively short exposure ages, it has been shown that GCR corrections can be significant for some samples (Hopkins *et al.*, 2019). Here we correct for production of ^{50}V in chondrites and thereby investigate the amount of V isotope variation in chondrites. We calculate the irradiation free V isotope compositions for 14 chondrites (Table S-2) and find that after correction for GCR effects there is no detectable variation within error among all the investigated samples, which is in agreement with conclusions from a previous study(Hopkins *et al.*, 2019). Given that the GCR corrected V isotope compositions of all carbonaceous, ordinary, enstatite and rumuruti chondrites are within error of each other, we calculate the error-weighted average chondritic V isotope composition to be $\delta^{51}V_{ch.}$ = -1.089 ± 0.029 ‰ (n = 14, 2SE). This value is identical to an unweighted average of all the data, which yields a value of -1.094 ± 0.030 ‰ (n = 14, 2SE).

It should be noted that there are significant uncertainties associated with correcting for GCR effects in general. In particular, the magnitude of GCR effects not only depends on the CRE age that is calculated based on noble gas isotope compositions of Ne, Ar or Kr, but also depends on the concentrations of potential target nuclei. Importantly, effects from neutron capture are not significant for vanadium (Hopkins *et al.*, 2019), which renders the comparison between CRE ages based on noble gases and V isotope anomalies more robust. However, in addition to Fe there are GCR spallation reactions that involve target nuclei of Ti and Cr that can lead to production of ^{50}V (Hopkins *et al.*, 2019). Because lunar rocks and chondrites can have very different abundances of Cr and, in particular, Ti, it is possible that application of the lunar GCR correction equation to chondrites is associated with a systematic error that would render the corrected chondrite average value incorrect. However, there are several reasons why such an effect, if present, does not significantly affect the average chondrite values calculated here. First, the corrections on chondrites are small (<0.3‰) and, therefore, the systematic error would have to be very large to impact corrected V isotope compositions. Second, theoretical calculations have shown that isotopes of Ti are the most likely alternative targets that can produce ^{50}V whereas the predicted effects from isotopes of Cr are likely negligible (Hopkins *et al.*, 2019). Chondrites uniformly have Ti concentrations around one order of magnitude or more lower than lunar rocks. Hence, if irradiation effects on Ti were significant then we would expect smaller associated corrections on chondrites than when using the GCR correction equation that only includes Fe as a target. For example, if we use (Fe+Ti)/V as a scaling factor in Fig. 1 instead of just Fe/V, then we obtain an error-weighted average GCR-corrected chondrite value of $\delta^{51}V_{ch.}$ = -1.137 ± 0.058‰ (2SE).

5. V isotope difference between the BSE, BSM and Chondrites

We carried out Monte Carlo simulations using the raw data for the BSM, BSE, and Chondrite data sets and their associated individual uncertainties to artificially generate 1 million datasets, and hence compute 1 million $\delta^{51}V$ mean values for the BSM, BSE, and Chondrites. The results of these simulations are shown in Figure S-6. These demonstrate that BSE is substantially heavier than both BSM and chondrites.

At each iteration step, the difference between the mean $\delta^{51}V$ of the BSM and Chondrites was computed as $\Delta^{51}V_{BSM\text{-}Chondrites} = \delta^{51}V_{BSM} - \delta^{51}V_{Chondrites}$. The distribution of $\Delta^{51}V_{BSM\text{-}Chondrites}$ values is shown in Figure S7, demonstrating that the probability for the BSM to have a higher mean $\delta^{51}V$ than Chondrites (i.e., $\Delta^{51}V_{BSM\text{-}chondrites} > 0$) is high (87.13%). These simulations demonstrate that a shift of 0.058 ± 0.051‰ (1SD) exists between the V isotope compositions of the BSM and Chondrites (Figure S-7). This is further substantiated by two-sample *t*-tests that return a test decision for the null hypothesis that the 1 million mean $\delta^{51}V$ values of the BSM and Chondrites come from independent random samples from normal distributions with equal means and equal but unknown variances. The alternative hypothesis is that these two data sets come from populations with unequal means. We carried out 100 two-sample *t*-tests for each time 1 million $\delta^{51}V$ values of the BSM and Chondrites and found that the null hypothesis was systematically rejected at the 5% significance level. This clearly demonstrates that the V isotope compositions of the BSM and Chondrites represent two populations with unequal means.

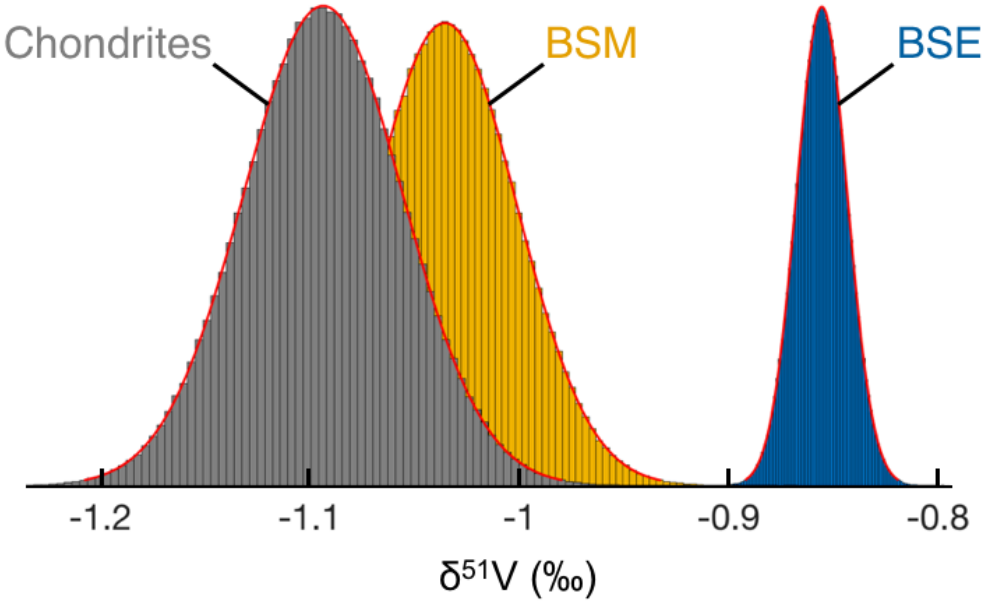

Figure S-6 Average V isotope compositions of chondrites, BSM, and BSE with their probability distributions based on 1 million Monte Carlo simulations of the available data (n= 14, 24 and 76 for Chondrites, BSM and BSE, respectively) and their associated 2SD error bars. Hence, the generated data populations take the full individual errors into account when generating the populations' averages. These show that BSE and BSM are both statistically more enriched in ^{51}V relative to chondrites.

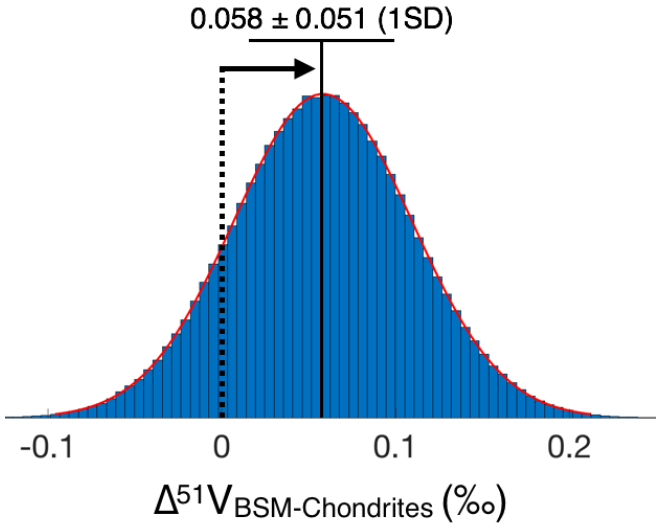

Figure S-7 Frequency distribution of the V isotope difference between the BSM and Chondrites ($\Delta^{51}V_{BSM\text{-}Chondrites}$) as generated by Monte Carlo simulations where the raw data and their associated uncertainties are used to artificially generate 1 million mean $\delta^{51}V_{BSM}$ and $\delta^{51}V_{Chondrites}$ values.

6. Assessment of vanadium depletion in bulk silicate Mars

Little previous quantitative work has been done to assess the extent of V depletion in BSM. Recently, Yoshizaki and McDonough (2020) used refractory lithophile element (RLE) ratio plots for martian meteorites to investigate whether these elements are present in chondritic proportions in BSM. They concluded that, similar to RLE, V was depleted in BSM relative to chondrites by not more ~10%. However, no details of this estimate were given. Here we follow the same approach as Yoshizaki and McDonough (2020) and construct two separate plots using V/Sc vs Y/Ca and V/Lu vs Yb/Ca. All elemental ratios are normalized to chondrites – considered as the bulk Mars composition – to tentatively assess the degree of V depletion in BSM (Fig. S8). In agreement with the analogous plots shown by Yoshizaki and McDonough (2020), the martian meteorite data exhibit significant scatter that may be due to a combination of factors such as analytical uncertainties, sample heterogeneity, fractional crystallization, and melting. However, it is notable that almost all martian meteorites exhibit lower V/Sc and V/Lu ratios than chondrites. Furthermore, if it is assumed that the two RLE ratios (i.e. Y/Ca and Yb/Ca) are present in BSM at the chondritic ratio (Yoshizaki and McDonough, 2020), then the intersection of the correlated data scatter with the chondritic Y/Ca and Yb/Ca ratios can be used to define a potential range of V/Sc (0.40–0.73) and V/Lu (0.37–0.77) in BSM relative to chondrites (Fig. S8). This approach hence enables a first-order assessment of V depletion in BSM, which results in a range of 27% to 60% based on the range of overlap between the V depletion estimates from V/Sc and V/Lu. It should be emphasized that this approach has its own limitations and it is not an attempt to provide a statistically robust best estimate for the V depletion in Mars, given the large scatter of the data. However, due to the almost uniform sub-chondritic V/Sc and V/Lu ratios in martian meteorites (Fig. S-8), it is highly likely that BSM is characterized by a significant V deficit relative to chondrite, which is best explained by V sequestration into the martian core.

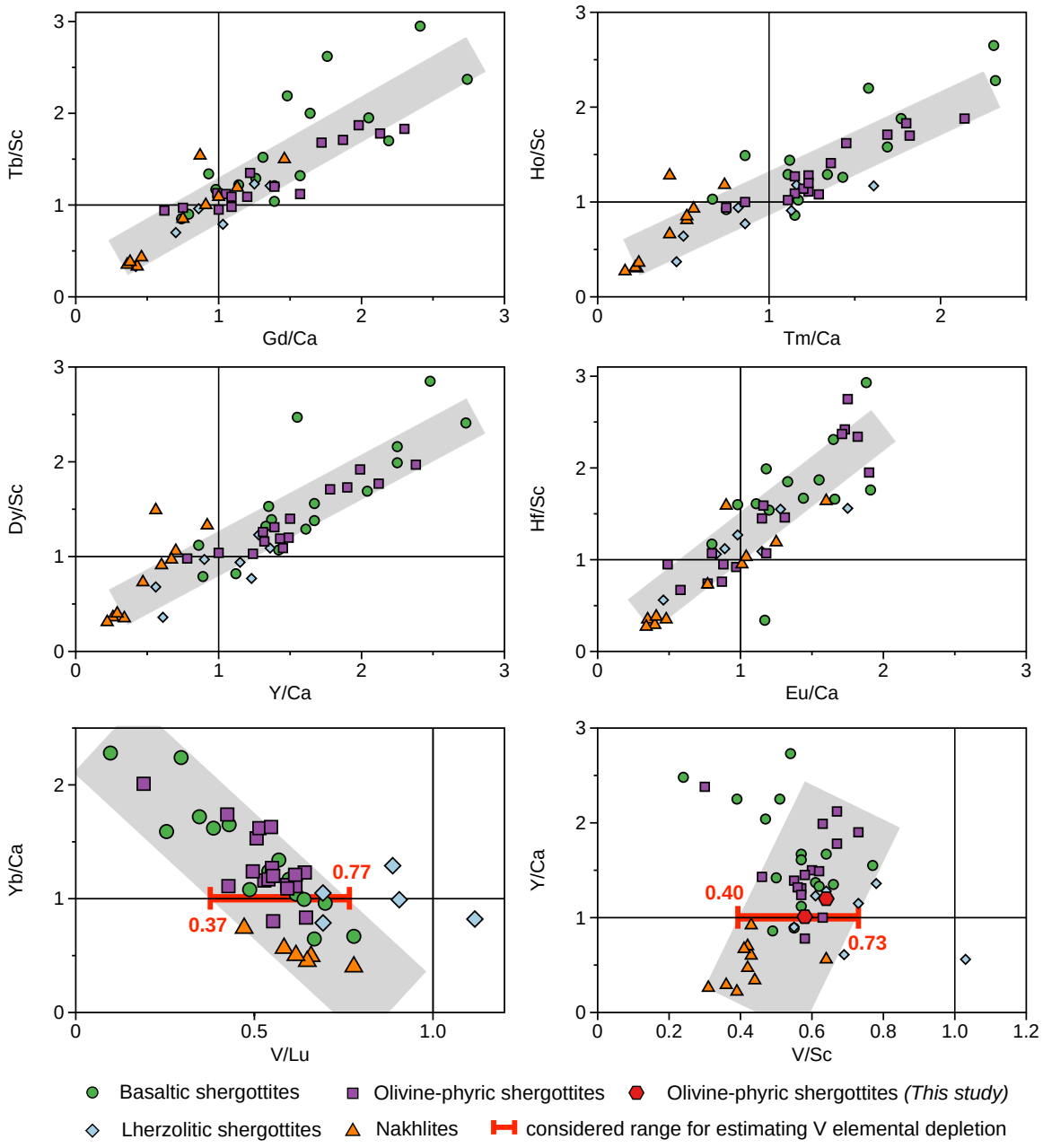

Figure S-8 Ratio/ratio plots of refractory lithophile elements in martian meteorites, normalized to CI chondrite abundances (Yoshizaki and McDonough, 2020). Chemical trend lines reflecting melt-residue differentiation in the martian silicate mantle, represented by the grey areas, appear to cross CI chondrite compositions for all elemental ratios except those involving V, hence pointing to a significant V depletion in martian meteorites relative to chondrites. Unless specified, data are from the compilation by Yoshizaki and McDonough, 2020.

Table S-1 V isotope data included in BSE estimate.

Sample name	Rock type	$\delta^{51}V$	error (2sd)[#]	references
	MORB			
HLY102D73	Basalt	-0.83	0.05	7
HLY102 D8	Basalt	-0.82	0.05	7
HLY102D26	Basalt	-0.81	0.07	7
HLY102D27	Basalt	-0.81	0.02	7
Vema33 D1-2	Basalt	-0.80	0.05	7
DR07-1	Basalt	-0.79	0.10	7
DR05-1	Basalt	-0.79	0.05	7
AII127D46-7	Basalt	-0.79	0.04	7
HLY102D38	Basalt	-0.76	0.06	7
2368-4	Basalt	-0.90	0.05	7
2737-8	Basalt	-0.89	0.05	7
2359-4	Basalt	-0.86	0.03	7
2392-9	Basalt	-0.86	0.10	7
2746-9	Basalt	-0.81	0.07	7
2746-14	Basalt	-0.79	0.09	7
264-04	Basalt	-0.96	0.10	7
265-05	Basalt	-0.93	0.10	7
265-113	Basalt	-0.86	0.08	7
J2-265-88	Basalt	-0.86	0.09	7
J265-82	Basalt	-0.85	0.02	7
266-33	Basalt	-0.84	0.04	7
266-01	Basalt	-0.82	0.09	7
265-49	Basalic andesite	-0.85	0.04	7
TR 16D 1g	Basalt	-1.04	0.15	3
MD57	Basalt	-0.99	0.09	3
POS210/1	Basalt	-0.97	0.22	3
TR30D 2g	Basalt	-0.96	0.05	3
TR 6D 2g	Basalt	-0.92	0.01	3
TR 15D 1g	Basalt	-0.84	0.15	3
	MORB Average (2SE)	-0.862	(0.026)	
	OIB			
BHVO-2	Hawaii	-0.86	0.10	9
BIR-1a	Iceland	-0.92	0.10	4,8,9
4567 45	Tholeiitic basalt Iceland	-1.00	0.07	3
408673	Tholeiitic basalt Iceland	-0.94	0.06	3
4567 49	Tholeiitic basalt Iceland	-0.93	0.10	3
4567 32	Tholeiitic basalt Iceland	-0.88	0.14	3
4567 40	Tholeiitic basalt Iceland	-0.85	0.10	3
4567 43	Tholeiitic basalt Iceland	-0.82	0.27	3
4567 14	Tholeiitic basalt Iceland	-0.82	0.12	3
4567 36	Tholeiitic basalt Iceland	-0.80	0.21	3
4567 22	Tholeiitic basalt Iceland	-0.75	0.26	3
	OIB Average (2SE)	-0.870	(0.044)	

	Komatiites/picrites			
89104	picrite	-0.8	0.01	4
89105/1	picrite	-0.76	0.04	4
9704	Ol-Px cumulate	-0.81	0.09	4
9705	Ol-Px cumulate	-0.82	0.06	4
91117	komatiite	-0.92	0.08	4
91106	komatiite	-0.86	0.05	4
TN2	komatiite	-0.95	0.08	4
TN10	komatiite	-0.9	0.02	4
ALX02	komatiite	-0.88	0.07	4
PH18	komatiite	-0.87	0.07	4
12-2	komatiite	-0.92	0.05	4
501-2	komatiite	-0.89	0.05	4
BV05	komatiite	-0.91	0.06	4
BV15	komatiite	-0.92	0.07	4
	Komatiite Average (2SE)	-0.872	(0.030)	
	Fresh peridotites			
S-37	spinel lherzolite	-0.91	0.03	4
S-21	spinel lherzolite	-0.90	0.10	4
S-14	spinel lherzolite	-0.93	0.05	4
S-4	spinel lherzolite	-0.85	0.04	4
S-15	spinel lherzolite	-0.91	0.07	4
S-17	spinel lherzolite	-0.90	0.09	4
S-2	spinel lherzolite	-0.93	0.04	4
S-1	spinel lherzolite	-0.95	0.04	4
S-22	spinel lherzolite	-0.92	0.03	4
S-16	spinel lherzolite	-0.92	0.05	4
H-25	Spinel Harzburgite	-0.93	0.03	4
313-1	garnet lherzolite	-0.72	0.15	3
313-6	garnet lherzolite	-0.62	0.15	3
313-102	garnet lherzolite	-0.58	0.07	3
313-104	garnet lherzolite	-0.83	0.22	3
313-106	garnet lherzolite	-0.75	0.03	3
313-112	garnet lherzolite	-0.70	0.15	3
BD 730	garnet lherzolite	-0.99	0.20	3
BD 822	spinel lherzolite	-0.78	0.15	3
314-56	spinel lherzolite	-0.77	0.15	3
314-58	spinel lherzolite	-0.81	0.29	3
Mo 101	spinel lherzolite	-0.64	0.09	3
	Peridotite Average (2SE)	-0.829	(0.050)	

[#] - error bars as reported in each manuscript. The long-term external errors often exceed what was reported for individual samples in these papers and it might be more appropriate to apply these. However, we have not weighted the samples used in the BSE estimate according to individual sample errors and the errors shown here are only for informational purposes.

Table S-2 Vanadium isotope compositions and GCR corrections for chondrites.

Sample	type	V* (µg/g)	Fe# (µg/g)	CRE age§ (Ma)	$\delta^{51}V_{meas}$¶	n	error (2sd)	$\delta^{51}V_{corr}$
EET92002	CK5	91	228042	33.1	-1.32	6	0.15	-1.14
Karoonda	CK4	91	237076	40.2	-1.32	9	0.07	-1.09
ALH83100	CM2	72	216146	0.17	-1.07	2	0.18	-1.07
Mighei	CM2	59	212400	2.2	-1.05	7	0.21	-1.03
DOM 08006	CO3.0	80	240717	19	-1.22	9	0.08	-1.10
Lance	CO3.5	76	236606	5	-1.22	9	0.26	-1.19
Warrenton	CO3.7	66	193920	34.2	-1.24	18	0.11	-1.03
St. Marks	EH5	51	320365	1.05	-1.05	4	0.10	-1.03
Indarch	EH4	50	290000	13.3	-1.39	2	0.15	-1.22
WSG95300	H3.3	66	254226	35	-1.39	3	0.07	-1.11
Borkut	L5	95	215000	12.4	-1.12	2	0.10	-1.06
Alfianello	L6	67	221257	28	-1.26	11	0.12	-1.06
Calliham	L6	65	215000	26	-1.32	2	0.10	-1.13
NWA753	R3.9	78	242899	11	-1.13	8	0.15	-1.05
					weighted average			-1.089
					weighted 2SE			0.029

* - All V concentration data are from (Nielsen *et al.*, 2019) except Indarch and Karoonda, which are from this study

- All Fe concentration data are from (Nielsen *et al.*, 2019) except Indarch, Calliham and Borkut that are group averages from (Wasson and Kallemeyn, 1988), Mighei that is from (Mason, 1963) and Karoonda that is from this study

¶ - All V isotope data are from (Nielsen *et al.*, 2019) except Indarch and Karoonda and four additional analyses of Alfianello, which are from this study

§ - CRE ages from (Mazor *et al.*, 1970; Sarafin *et al.*, 1984; Alexeev, 1998; Wieler *et al.*, 1999; Scherer and Schultz, 2000; Patzer and Schultz, 2001; Schultz *et al.*, 2005; Davidson *et al.*, 2019; Hopkins *et al.*, 2019)

Supplementary Information References

Alexeev, V.A. (1998) Parent bodies of L and H chondrites: Times of catastrophic events. *Meteoritics & Planetary Science* 33, 145-152.

Davidson, J., Alexander, C.M.O.D., Stroud, R.M., Busemann, H., Nittler, L.R. (2019) Mineralogy and petrology of Dominion Range 08006: A very primitive CO3 carbonaceous chondrite. *Geochimica Et Cosmochimica Acta* 265, 259-278.

Hopkins, S.S., Prytulak, J., Barling, J., Russell, S.S., Coles, B.J., Halliday, A.N. (2019) The vanadium isotopic composition of lunar basalts. *Earth and Planetary Science Letters* 511, 12-24.

Mason, B. (1963) The carbonaceous chondrites. *Space Science Reviews* 1, 621-646.

Mazor, E., Heymann, D., Anders, E. (1970) Noble gases in carbonaceous chondrites. *Geochimica Et Cosmochimica Acta* 34, 781-824.

Nielsen, S.G., Auro, M., Righter, K., Davis, D., Prytulak, J., Wu, F., Owens, J.D. (2019) Nucleosynthetic vanadium isotope heterogeneity of the early solar system recorded in chondritic meteorites. *Earth and Planetary Science Letters* 505, 131-140.

Nielsen, S.G., Owens, J.D., Horner, T.J. (2016) Analysis of high-precision vanadium isotope ratios by medium resolution MC-ICP-MS. *Journal of Analytical Atomic Spectrometry* 31, 531-536.

Nielsen, S.G., Prytulak, J., Halliday, A.N. (2011) Determination of Precise and Accurate 51V / 50V Isotope Ratios by MC-ICP-MS, Part 1: Chemical Separation of Vanadium and Mass Spectrometric Protocols. *Geostandards and Geoanalytical Research* 35, 293-306.

Nyquist, L.E., Bogard, D.D., Shih, C.-Y., Greshake, A., Stöffler, D., Eugster, O. (2001) Ages and Geologic Histories of Martian Meteorites. *Space Science Reviews* 96, 105-164.

Patzer, A., Schultz, L. (2001) Noble gases in enstatite chondrites I: Exposure ages, pairing, and weathering effects. *Meteoritics & Planetary Science* 36, 947-961.

Prytulak, J., Nielsen, S.G., Halliday, A.N. (2011) Determination of Precise and Accurate 51V / 50V Isotope Ratios by Multi-Collector ICP-MS, Part 2: Isotopic Composition of Six Reference Materials plus the Allende Chondrite and Verification Tests. *Geostandards and Geoanalytical Research* 35, 307-318.

Prytulak, J., Nielsen, S.G., Ionov, D.A., Halliday, A.N., Harvey, J., Kelley, K.A., Niu, Y., Peate, D.W., Shimizu, K., Sims, K.W.W. (2013) The Stable Vanadium Isotope Composition of the Mantle and Mafic Lavas. *Earth and Planetary Science Letters* 365, 177-189.

Prytulak, J., Sossi, P.A., Halliday, A.N., Plank, T., Savage, P.S., Woodhead, J.D. (2017) Stable vanadium isotopes as a redox proxy in magmatic systems? *Geochemical Perspectives Letters* 3, 75-84.

Qi, Y.H., Wu, F., Ionov, D.A., Puchtel, I.S., Carlson, R.W., Nicklas, R.W., Yu, H.M., Kang, J.T., Li, C.H., Huang, F. (2019) The vanadium isotopic composition of the BSE: constraints from peridotites and komatiites. *Geochimica Et Cosmochimica Acta* 259, 288-301.

Rizo, H., Walker, R.J., Carlson, R.W., Horan, M.F., Mukhopadhyay, S., Manthos, V., Francis, D., Jackson, M.G. (2016) Preservation of Earth-forming events in the tungsten isotopic composition of modern flood basalts. *Science* 352, 809-812.

Sarafin, R., Bonani, G., Herpers, U., Signer, P., Hofmann, H., Nessi, M., Morenzoni, E., Suter, M., Wieler, R., Wölfli, W. (1984) Spallogenic nuclides in meteorites by conventional and accelerator mass spectrometry. *Nuclear Instruments and Methods in Physics Research Section B: Beam Interactions with Materials and Atoms* 5, 411-414.

Scherer, P., Schultz, L. (2000) Noble gas record, collisional history, and pairing of CV, CO, CK, and other carbonaceous chondrites. *Meteoritics & Planetary Science* 35, 145-153.

Schultz, L., Weber, H.W., Franke, L. (2005) Rumuruti chondrites: Noble gases, exposure ages, pairing, and parent body history. *Meteoritics & Planetary Science* 40, 557-571.

Schuth, S., Horn, I., Bruske, A., Wolff, P.E., Weyer, S. (2017) First vanadium isotope analyses of V-rich minerals by femtosecond laser ablation and solution-nebulization MC-ICP-MS. *Ore Geology Reviews* 81, 1271-1286.

Sossi, P.A., Moynier, F., Chaussidon, M., Villeneuve, J., Kato, C., Gounelle, M. (2017) Early Solar System irradiation quantified by linked vanadium and beryllium isotope variations in meteorites. *Nature Astronomy* 1, 0055.

Sossi, P.A., Prytulak, J., O'Neill, H.S.C. (2018) Experimental calibration of vanadium partitioning and stable isotope fractionation between hydrous granitic melt and magnetite at 800C and 0.5 GPa. *Contributions to Mineralogy and Petrology* 173.

Wasson, J.T., Kallemeyn, G.W. (1988) Compositions of chondrites. *Phil. Trans. R. Soc. Lond. Ser. A* 325, 535-544.

Wieler, R., Baur, H., Busemann, H., Heber, V.S., Leya, I. (1999) Noble Gases in Desert Meteorites: Howardities, Unequilibrated Chondrites, Regolith Breccias and an LL7*Workshop on Extraterrestrial Materials from Cold and Hot Deserts*, Pilanesberg, South Africa.

Wu, F., Owens, J.D., Huang, T., Sarafian, A., Huang, K.-F., Sen, I.S., Horner, T.J., Blusztajn, J., Morton, P., Nielsen, S.G. (2019) Vanadium Isotope Composition of Seawater. *Geochimica Et Cosmochimica Acta* 244, 403-415.

Wu, F., Qi, Y., Perfit, M.R., Gao, Y., Langmuir, C.H., Wanless, V.D., Yu, H., Huang, F. (2018) Vanadium isotope compositions of mid-ocean ridge lavas and altered oceanic crust. *Earth and Planetary Science Letters* 493, 128-139.

Wu, F., Qi, Y.H., Yu, H.M., Tian, S.Y., Hou, Z.H., Huang, F. (2016) Vanadium isotope measurement by MC-ICP-MS. *Chemical Geology* 421, 17-25.

Yoshizaki, T., McDonough, W.F. (2020) The composition of Mars. *Geochimica Et Cosmochimica Acta* 273, 137-162.